UNCERTAINTY IN THE SPECIFICATION OF SURFACE CHARACTERISTICS: A STUDY OF PREDICTION ERRORS IN THE BOUNDARY LAYER

KIRAN ALAPATY[1,*] SETHU RAMAN[2] and DEVDUTTA S. NIYOGI[2]
[1]*Environmental Programs, MCNC-North Carolina Supercomputing Center, Research Triangle Park, North Carolina, U.S.A. and* [2]*Department of Marine, Earth and Atmospheric Sciences, North Carolina State University, Raleigh , North Carolina, U.S.A.*

(Received in final form 26 August, 1996)

Abstract. The effects of uncertainty in the specification of surface characteristics on simulated atmospheric boundary layer (ABL) processes and structure were investigated using a one-dimensional soil-vegetation-boundary layer model. Observational data from the First International Satellite Land Surface Climatology Project Field Experiment were selected to quantify prediction errors in simulated boundary-layer parameters. Several numerical 12-hour simulations were performed to simulate the convective boundary-layer structure, starting at 0700 LT 6 June 1987.

In the control simulation, measured surface parameters and atmospheric data were used to simulate observed boundary-layer processes. In the remaining simulations, five surface parameters – soil texture, initial soil moisture, minimum stomatal resistance, leaf area index, and vegetation cover – were varied systematically to study how uncertainty in the specification of these surface parameters affects simulated boundary-layer processes.

The simulated uncertainty in the specification of these five surface parameters resulted in a wide range of errors in the prediction of turbulent fluxes, mean thermodynamic structure, and the depth of the ABL. Under certain conditions uncertainty in the specifications of soil texture and minimum stomatal resistance had the greatest influence on the boundary-layer structure. A lesser but still moderately strong effect on the simulated ABL resulted from (1) a small decrease (4%) in the observed initial soil moisture (although a large increase [40%] had only a marginal effect), and (2) a large reduction (66%) in the observed vegetation cover. High uncertainty in the specification of leaf area index had only a marginal impact on the simulated ABL. It was also found that the variations in these five surface parameters had a negligible effect on the simulated horizontal wind fields. On the other hand, these variations had a significant effect on the vertical distribution of turbulent heat fluxes, and on the predicted maximum boundary-layer depth, which varied from about 1400–2300 m across the 11 simulations. Thus, uncertainties in the specification of surface parameters can significantly affect the simulated boundary-layer structure in terms of meteorological and air quality model predictions.

Key words: Uncertainty, boundary layer, surface characteristics, prediction errors.

1. Introduction

There are several sophisticated soil-vegetation parameterization schemes that provide realistic representations of land surface-atmosphere exchange processes in meteorological models. However, using these comprehensive schemes requires

[*] *Corresponding author address*: Dr. Kiran Alapaty, Environmental Programs, MCNC-North Carolina Supercomputing Center, P.O. Box 12889, 3021 Cornwallis Road, Research Triangle Park, NC 27709-2889. E-mail: alapaty@flyer.ncsc.org

Boundary-Layer Meteorology **82:** 473–500, 1997.

specifying many input parameters to properly represent the characteristics of the land surface. The lack of these data for use in three-dimensional meteorological models has been a major hindrance in the ability to use complex soil-vegetation schemes with a high degree of confidence. For example, proper specification of soil moisture in meteorological models, particularly for short-range weather forecasts, is important because it can influence the surface energy balance. The magnitude of the predicted turbulent sensible heat flux is modulated by the soil moisture through the release of turbulent latent heat flux from bare soil and/or canopy, affecting the kinetic energy of the turbulent eddies. Thus, soil moisture is one of the surface parameters that regulates the surface energy balance and hence the structure of the atmospheric boundary layer (ABL). However, because observed soil moisture data are not readily available for use in research and operational meteorological models, it is not possible to determine how well estimates of initial soil moisture represent existing conditions.

The input data to be specified depend on the type of soil-vegetation scheme used in a model. For example, if a meteorological model uses a simple climatological soil moisture parameterization (e.g., Anthes et al., 1987), then one need only specify the land use type in the modelled domain to allow interaction between the surface and the atmosphere. On the other hand, if a meteorological model uses the Biosphere-Atmosphere Transfer Scheme (Dickinson et al., 1993), then the number of input data to be specified in describing the characteristics of the modelled land surface increases dramatically. The situation is further complicated because measurements for many of these required input parameters are not available for use in three-dimensional meteorological modelling. Thus, many meteorological models using soil-vegetation schemes rely on empirical formulations (e.g., Dickinson et al., 1993) to prepare time-dependent and time-independent surface data. However, using these empirical formulations in meteorological models is questionable because observational data are not available for validation. Thus, empirical estimates of surface data may contain uncertainties in describing the spatial characteristics of the land surface.

Several studies have shown that variations in surface characteristics affect the prediction of near-surface turbulent fluxes in the ABL, and that variations in the turbulent fluxes influence the prediction of ABL structure. Deardorff (1978) showed that vegetation and soil moisture effects significantly alter surface parameters such as temperature and turbulent fluxes. McCumber and Pielke (1981) found that vegetation and the soil moisture distribution affect the mesoscale circulation patterns, thus affecting model predictions of precipitation and other meteorological features. Sellers et al. (1986) and Dickinson et al. (1993) have shown the importance of including biospheric schemes in global models. Pitman et al. (1990), Anthes (1984), and Sud and Smith (1985) found that including vegetation forcings in the models produced changes in the precipitation patterns.

Wetzel and Chang (1987, 1988) and Kim and Stricker (1996) showed that soil properties profoundly affect model predictions. Using the concept of effective

parameters for subgrid heterogeneity, Noilhan and Lacarrere (1995) showed that surface parameters such as soil texture and minimum stomatal resistance need special consideration in their representation to reduce prediction errors. The impact and errors associated with soil parameterizations were also highlighted by Ek and Cuenca (1994). Similarly, from the global modelling perspective, Pitman (1994) has demonstrated the impact of surface parameters for forest and grasslands using a single-column model. Using SiB (Sellers et al., 1986) in a columnar atmospheric model, da Rocha et al. (1996) studied Amazonian deforestation using appropriate vegetation and surface hydrological representations. Mihailovic et al. (1992) used observations over a maize field to show that the fractional vegetation cover and soil texture alter the diurnal forcings of meteorological parameters.

At mesoscale resolutions, Jacquemin and Noilhan (1990) performed a sensitivity study using the HAPEX-MOBILHY observations (André et al., 1986). They found the following order of importance for surface parameters: soil moisture, vegetation cover, minimum stomatal resistance, leaf area index, and surface roughness. However, Jacobs and DeBruin (1992) and Pitman (1994) have asserted that coupled studies are required to properly account for feedback between the surface and the atmosphere. Similarly, studies such as Henderson-Sellers (1993) and Niyogi et al. (1996) have shown the importance of including interactions in biospheric-atmospheric simulations. Their studies suggest that the feedback errors from various parameters are interactive. Mascart et al. (1991) identified the roles of various parameters that interactively determine the response of a parameter such as stomatal resistance.

Thus, a number of studies have documented the sensitivity of ABL and mesoscale circulations to variations in the surface characteristics. However, they did not quantify the prediction errors in the ABL that resulted from the uncertainties in the specification of surface characteristics as a feedback mechanism. Special observational data, such as those from the First International Satellite Land Surface Climatology Project (ISLSCP) Field Experiment (FIFE) (Sellers et al., 1992), provide a unique opportunity to quantify prediction errors resulting from these uncertainties. This can be achieved by varying the surface characteristics in simulations of the structures of the ABL.

The objectives of this research are (1) to study the effects of uncertainty in the specification of surface characteristics; (2) to quantify the resulting prediction errors, by simulating the structure of a convective boundary layer using a one-dimensional (1-D) soil-vegetation-boundary-layer model; and (3) to identify the parameters that have the most influence on the predicted boundary-layer structure.

2. The Model

We use a windowed soil-vegetation-boundary-layer model developed by Alapaty et al. (1996) to simulate boundary-layer structures over the FIFE area. This model

has 35 vertical sigma layers and 3×3 grid cells in the horizontal. Essentially, this is a 1-D model in which predictions are made only at the central grid cell [2,2] for all the vertical layers. There are two possible ways to use this model for numerical simulations-horizontal and vertical advection of prognostic variables can be included, or spatial advection can be neglected. In the present study, we use the second option. The governing equations and a brief description of the parameterization schemes used in this study are given below. For further details, see Alapaty et al. (1996).

2.1. THE GOVERNING EQUATIONS

The prognostic equations for any layer i in the model atmosphere can be written as

$$\frac{\partial u_i}{\partial t} = -\sum_{j=1}^{N} C_{ij}(t, \Delta t) u_j(t) + f(v_i - V_i) \tag{1}$$

$$\frac{\partial v_i}{\partial t} = -\sum_{j=1}^{N} C_{ij}(t, \Delta t) v_j(t) + f(u_i - \psi_i) \tag{2}$$

$$\frac{\partial T_i}{\partial t} = -\sum_{j=1}^{N} C_{ij}(t, \Delta t) T_i(t) \tag{3}$$

$$\frac{\partial q_i}{\partial t} = -\sum_{j=1}^{N} C_{ij}(t, \Delta t) q_i(t) \tag{4}$$

where u and v are the eastward and northward components of the wind, respectively, C is called the transilient matrix, the subscripts i and j are indices of two different layers in a column of atmosphere, t is time, and Δt is the time step used in the numerical integration, f is the Coriolis parameter, ψ and V are the eastward and northward geostrophic winds, respectively, T is temperature; and q is the mixing ratio of water vapour. In the above diffusion Equations (1)–(4), local vertical gradients of turbulent fluxes are replaced by respective mixing terms to represent the effects of nonlocal subgrid-scale vertical mixing.

The soil-vegetation parameterization scheme used in this model was suggested by Noilhan and Planton (1989) and Jacquemin and Noilhan (1990). There are two soil layers, to represent the surface and subsurface processes; layer 1 is 0.01 m thick and layer 2 is 1 m thick. The prognostic equations to calculate the mean temperatures of these two layers can be written as

$$\frac{\partial T_{g1}}{\partial t} = C_T(R_n - S_{hf} - L_{hf}) - \frac{2\pi}{\tau}(T_{g1} - T_{g2}) \tag{5}$$

$$\frac{\partial T_{g2}}{\partial t} = \frac{1}{\tau}(T_{g1} - T_{g2}) \tag{6}$$

where T_{g1} and T_{g2} are the temperatures of layers 1 and 2, C_T is the inverse of the thermal capacity of a particular soil type, R_n is the net radiation at the surface, S_{hf} and L_{hf} are the surface turbulent sensible and latent heat fluxes, and τ is a time constant, equal to the number of seconds in a day.

The prognostic equations for the mean soil moisture for the two layers are given as

$$\frac{\partial W_{g1}}{\partial t} = \frac{C_1}{\rho_w d_1}(P_g - E_g) - \frac{C_2}{\tau}(W_{g1} - W_{geq}) \tag{7}$$

$$\frac{\partial W_{g2}}{\partial t} = \frac{1}{\rho_w d_2}(P_g - E_g - E_{tr}) \tag{8}$$

where W_{g1} and W_{g2} are the mean volumetric soil moisture contents for layers 1 and 2, C_1 and C_2 are soil moisture coefficients, ρ_w is the density of liquid water, d_1 and d_2 are the thicknesses of the two soil layers, P_g is the flux of liquid water reaching the soil surface, E_g is the evaporation at the soil surface, W_{geq} is the layer 1 soil moisture when gravity balances the capillary forces, and E_{tr} is the transpiration rate. For further details, see Noilhan and Planton (1989) and Jacquemin and Noilhan (1990).

The water content on the wet parts of the canopy due to rainfall and/or dew formation on the foliage is represented by W_r. The prognostic equation for W_r is given based on Deardorff's formulation (1978) and it can be written as

$$\frac{\partial W_r}{\partial t} = (V_c P_r) - E_r \tag{9}$$

where V_c is the vegetation cover in fractional units, P_r is the precipitation rate at the top of the vegetation, and E_r is the evapouration rate from the wet parts of the canopy.

A simple radiation model is considered in this study. Net radiation at the surface (R_n) is calculated as the sum of incoming solar radiation absorbed at the surface (I_S), atmospheric downwards and outgoing longwave surface radiation

$$R_n = I_S + I_L.$$

Here I_S is estimated as

$$I_S = S\cos Z(1 - A)b^{\sec Z}$$

where S is the solar constant, Z the solar zenith angle, A the surface albedo, and b the atmospheric turbidity. I_L, the net longwave irradiance, is computed as

$$I_L = I_{Ld} - I_{Lu}$$

where I_{Lu} and I_{Ld} are outgoing and downward longwave radiation. These can be written as (Anthes et al., 1987):

$$I_{Lu} = \epsilon_g \sigma_S T_{g1}^4$$

$$I_{Ld} = \epsilon_g \epsilon_a \sigma_S T_a^4$$

where ϵ_g is the soil emissivity, σ_S is the Stefan-Boltzmann constant, ϵ_a is the atmospheric longwave emissivity ($\epsilon_a = 0.725 + 0.17\log_{10} W_p$, where W_p is the precipitable water in centimeters), and T_a is the atmospheric temperature at a sigma level approximately 40 hPa above the surface.

2.2. BOUNDARY-LAYER FORMULATION

The lower boundary layer (the surface layer) is parameterized based on similarity theory suggested by Monin and Yaglom (1971). The nondimensional functions can be written as

$$\frac{kz}{u_*}\frac{\partial u}{\partial z} = \Phi_m(z/L)$$

$$\frac{kz}{\theta_*}\frac{\partial \Theta}{\partial z} = \Phi_h(z/L)$$

$$\frac{kz}{q_*}\frac{\partial q}{\partial z} = \Phi_q(z/L)$$

where k is the von Karman constant, z is altitude, u_* is friction velocity, θ_* and q_* are scales for temperature and water vapour, Θ is potential temperature, and the nondimensional stability parameters Φ_m, Φ_h, and Φ_q for momentum, heat, and moisture are functions of the Obukhov length, L (Businger et al., 1971). Sensible heat fluxes are computed using the relationship given by

$$S_{hf} = u_* \theta_* \tag{10}$$

and latent heat fluxes are computed from the soil-vegetation model, where bare ground evapouration and evaporation from transpiring canopies and wet parts of the canopies (due to dew formation or rainfall interception) are estimated. Thus, the total latent heat flux at the surface can be written as

$$L_{hf} = E_g + E_{tr} + E_r \tag{11}$$

where E_g, E_{tr}, and E_r are defined as in the previous subsection.

Mixed-layer processes are represented using a nonlocal-closure mixed-layer scheme, the transilient turbulence parameterization scheme (Stull and Driedonks,

1987). Let S be any variable such as the potential temperature or horizontal wind components or mixing ratio of water vapour in the atmosphere. The new value of S due to subgrid-scale turbulent vertical mixing for a grid cell i at a future time $(t + \Delta t)$ can be written as

$$S_i(t + \Delta t) = \sum_{j=1}^{N} C_{ij}(t, \Delta t) S_j(t) \tag{12}$$

where C is the transilient matrix and the subscripts i and j are indices of two different grid cells in a column of atmosphere. For turbulent mixing between grid cells i and j, C_{ij} represents the fraction of air mass ending in grid cell i that came from grid cell j; cell i is considered the "destination" cell and cell j is considered the "source" cell. Thus, the change in S due to subgrid-scale vertical mixing for grid cell i after a time interval Δt is a simple matrix multiplication with its source cell. Estimation of the transilient matrix is the closure problem in this parameterization. This can be solved by considering the turbulent kinetic energy (TKE) equation in a simplified form:

$$\frac{\partial E}{\partial t} = -\overline{u'w'}\frac{\partial u}{\partial z} - \overline{v'w'}\frac{\partial v}{\partial z} + \frac{g}{\overline{\Theta}_v}\overline{w'\theta'_v} - \epsilon \tag{13}$$

where E is the TKE per unit mass, u and v are horizontal wind components, g is the acceleration due to gravity, and $\overline{\Theta}_v$ is the mean virtual potential temperature. On the right side of this equation, the first and second terms are shear production terms, the third term is buoyancy production, and ϵ is the rate of TKE dissipation. After normalizing with E and representing turbulent flux terms in terms of known dynamic and thermodynamic parameters, the finite difference form of Equation (13) can be written as (Stull and Driedonks, 1987):

$$Y_{ij} = \frac{T_o \Delta t}{(\Delta z)^2_{ij}} \left[(\Delta u)^2_{ij} + (\Delta v)^2_{ij} - \left(\frac{g}{R_c \Theta_{vi}} \right) (\Delta \Theta_v)_{ij} (\Delta z)_{ij} \right] - \frac{\Delta t D}{T_o} \tag{14}$$

where Y_{ij} is called the mixing potential, T_o is the time scale of turbulence, the terms including Δ are the respective parametric differences between cells i and j, R_c is the critical Richardson number, and D is the turbulence dissipation factor. Then, the transilient matrix C_{ij} can be written as

$$C_{ij} = \frac{m_j Y_{ij}}{\mid Y \mid_\infty} \qquad \text{for } i \neq j$$

where m_j is the mass of air in cell j, and $\mid Y \mid_\infty$ is called the L_∞ norm of matrix Y. The diagonal elements (for $i = j$) of the transilient matrix can be written as

$$C_{ii} = 1 - \sum_{\substack{j=1 \\ i \neq j}}^{N} C_{ij}$$

The vertical turbulent fluxes, F, at any layer interface can be obtained from the following finite difference equation (Stull and Driedonks, 1987):

$$F_k(t, \Delta t) = F_{k-1} + \frac{\Delta z}{\Delta t} \sum_{j=1}^{N} C_{ij}(t, \Delta t)[S_k(t) - S_j(t)] \tag{15}$$

where k is the vertical layer index. When $k = 1$, $F_0 = 0$, since there are no turbulent fluxes through the ground.

3. Input Data and Numerical Simulations

Observational FIFE data were used to perform the numerical simulations. The FIFE site was located near Manhattan, Kansas, covering 15×15 km^2 where grass prairie was the predominant vegetation. Of the five intensive field campaigns (IFCs) from the FIFE data (Sellers et al., 1992), we selected measurements from the first IFC to provide initial conditions and to compare with the model simulations. During these IFCs, special efforts were made to measure various meteorological, hydrological, and biological parameters. The starting time of numerical simulations is 0700 LT 6 June 1987. Clear sky conditions were noticed during this day, which was listed as one of the "Golden Days" (Sellers et al., 1992). The geostrophic winds used in this study are same as those used by Alapaty et al. (1996).

There is spatial heterogeneity in the measured values of some of the surface parameters (e.g., initial soil moisture, leaf area index, roughness length) within the FIFE region. There are also differences in the measured values of a single parameter using different measurement techniques. Thus, the prepared initial conditions data for these surface parameters (Table I) include some uncertainty. To minimize this uncertainty, we matched surface data for initial conditions with those used in other studies reported in the literature (contained within Sellers et al., 1992).

We performed several numerical simulations to study how uncertainty in the specification of surface characteristics affected the predicted boundary-layer structure. The control simulation, which used observed surface characteristics, was performed and reported previously by Alapaty et al. (1996). In the remaining simulations, we systematically varied five surface parameters: soil texture, initial soil moisture, minimum stomatal resistance, leaf area index, and vegetation cover. In all cases, numerical simulations were performed for 12 daytime hours to simulate the convective boundary-layer processes.

4. Results and Discussion

For each of the simulations, we compare predicted turbulent heat fluxes, vertical profiles of temperature, water vapour mixing ratio, and horizontal winds with the

Table I
Surface parameter values used in the control (case 1) simulation

Parameter	Abbreviation	Value used
Minimum stomatal resistance	$R_{s\,\min}$	60.0 s m^{-1}
Leaf area index	LAI	1.90
Vegetation cover	Veg	0.99
Soil texture	–	Silty clay loam
Layer 1 volumetric soil moisture	W_{g1}	0.23 m^3 m^{-3}
Layer 2 volumetric soil moisture	W_{g2}	0.25 m^3 m^{-3}
Surface roughness length	Z_o	0.045 m
Layer 1 soil temperature	T_{g1}	298.15 K
Layer 2 soil temperature	T_{g2}	293.35 K

Table II
Specified surface characteristics in uncertainty study simulations

Parameter specified	Simulation identification	Type/value used
Soil texture	Case 1	Silty clay loam (observations)
	Case 2	Loamy sand
	Case 3	Clay
Initial soil moisture (m^3 m^{-3})	Case 1	0.230 (layer 1) and 0.250 (layer 2) (observations)
	Case 4	0.322 (field capacity)
	Case 5	0.240 ($\sim$10% higher than wilting point)
Minimum stomatal resistance (s m^{-1})	Case 1	60 (tall grass) (observations)
	Case 6	40 (maize)
	Case 7	450 (oats)
Leaf area index	Case 1	1.9 (observations)
	Case 8	1.0 (meadows)
	Case 9	3.0 (farmlands)
Vegetation cover	Case 1	0.99 (observations)
	Case 10	0.66
	Case 11	0.33

observations. Table II shows the list of numerical simulations (11 total cases) and specifies the variations in the five surface parameters.

4.1. SOIL TEXTURE

One type of input data to the soil-vegetation scheme (Noilhan and Planton, 1989) is the soil texture for the modelled land surface. For a coarser soil, such as loamy sand, hydraulic diffusivity and conductivity are higher than in a finer soil, such as clay; thus, soil texture affects water flow in the soil. Further, each soil texture has a

different water holding (water retention) capacity. Several studies have shown that soil texture plays a crucial role in controlling the structure of the ABL. Noilhan and Lacarrere (1995) found that soil texture has the highest impact in terms of effective grid representativeness for mesoscale predictions. Similarly, Pitman (1994) showed that soil texture representation directly affects surface temperature and runoff predictions. Mihailovic et al. (1992) found two regimes of surface latent heat flux variability. In the first regime, predicted latent heat fluxes over finer textured soil surfaces (from loamy sand to silt loam) are less sensitive to vegetation cover, and leaf area index. In the other regime, predicted latent heat fluxes over coarser texture soil surfaces (from loam to silty clay) are more sensitive to vegetation cover, and leaf area index. Mahfouf et al. (1987) also found that soil texture had a large influence on their model simulations.

Therefore, proper specification of soil texture is important in numerical simulation studies. In case 1, which is the control simulation, observed surface characteristics were used to simulate the temporal structures of the ABL. To demonstrate how uncertainty in the specification of soil texture affects the prediction errors in simulating boundary-layer processes, we performed simulation case 2 and case 3. In case 2 we used a coarser soil (loamy sand), while in case 3 we used a finer soil (clay). The other surface parameters, including initial soil moisture, remained constant in cases 1 through 3.

Figure 1a shows the temporal variations in observed and predicted turbulent latent heat fluxes. Predicted turbulent latent heat fluxes in case 1 (control simulation) are close to the observations, while those in case 2 are higher by $\sim$0–40 W m^{-2}. Since loamy sand (case 2) is coarser than silty clay loam soil (case 1), the case 2 soil hydraulic diffusivity and conductivity are higher than in case 1. Therefore, more water is available in the top layer of soil, resulting in case 2 having a larger latent heat flux than case 1 and the observations. The budget of the total turbulent latent heat flux (Equation (11)) in cases 1 and 2 indicates that $\sim$80% of the total latent heat flux comes from evapotranspiration while only $\sim$20% comes from bare soil evaporation. In case 3, the predicted latent heat flux is significantly lower than in the observations; the maximum in case 3 (100 W m^{-2}) is about four times lower than in the observations (400 W m^{-2}). This occurs because the case 3 initial soil moisture in the second soil layer is lower than the wilting point value for clay, so evapotranspiration is at a minimum, accounting for only $\sim$20% of the total latent heat flux. Most of the latent heat flux in case 3 ($\sim$80%) comes from bare soil evaporation.

The temporal variations in observed and predicted turbulent sensible heat fluxes for cases 1 through 3 are shown in Figure 1b. The effects of differences in the predicted latent heat fluxes are clearly reflected in an opposite trend in the respective predicted sensible heat fluxes. Sensible heat fluxes in case 1 are close to the observations, while in case 2 they are lower by 30 W m^{-2}. Sensible heat fluxes in case 3 are significantly higher than those in the observations, case 1, and case 2.

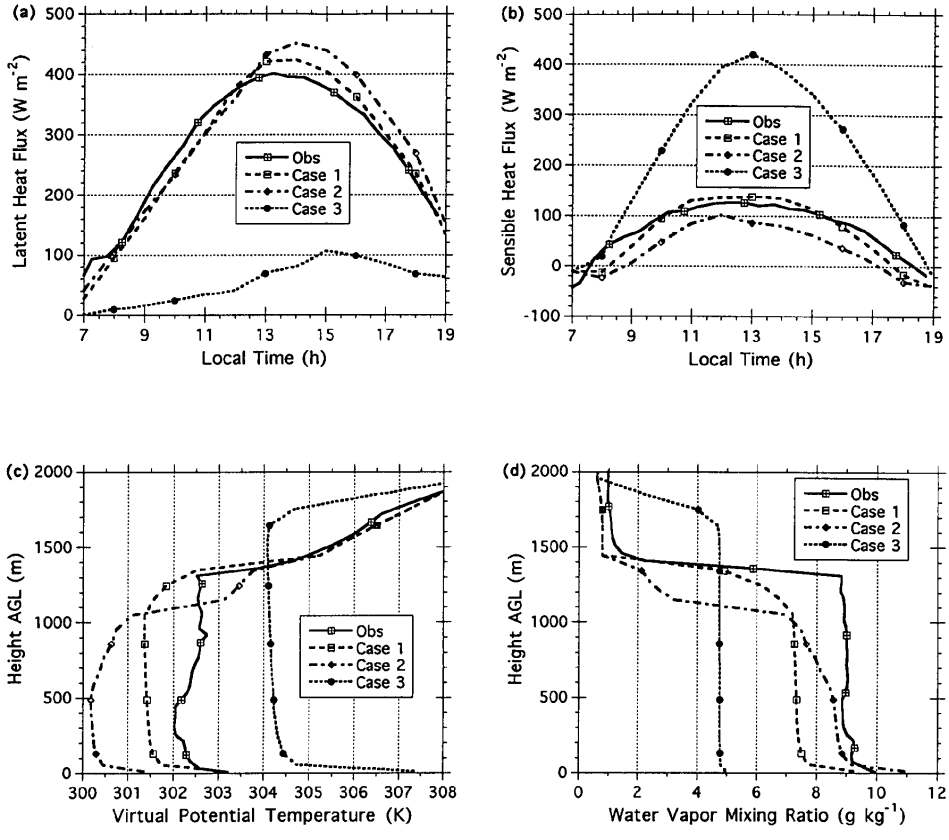

Figure 1. Observations and predictions for the soil texture study: (a) temporal variation in turbulent latent heat fluxes, (b) temporal variation in turbulent sensible heat fluxes, (c) vertical variation in virtual potential temperature at 1300 LT, and (d) vertical variation in water vapour mixing ratio at 1300 LT.

The maximum sensible heat flux in case 3 is about three times higher than in the observations.

Figure 1c shows the vertical distribution of "observed" virtual potential temperature (Θ_v) (estimated from the observed temperature and water vapour mixing ratio) and those predicted in cases 1 through 3 at 1300 LT. The observed vertical distribution of Θ_v indicates the presence of superadiabatic lapse rates in the surface layer. Vertical gradients in the observed Θ_v profile in the mixed layer between altitudes 500 and 1300 m indicate the advection of warmer air to the observational site (Sellers et al., 1992). Note that the predicted Θ_v in case 1 (control simulation) is lower than the observations by 1.25 K. This may be attributable to (1) the neglect of horizontal advection in the model simulations and/or (2) the presence of some uncertainty in the surface data for initial conditions. Cases 2 and 3 show predicted Θ_v distributions that are farther from the observations. In case 2, predicted turbulent

latent heat fluxes are larger and sensible heat fluxes smaller than in the observations and case 1, resulting in a case 2 mean Θ_v in the mixed layer that is 2 K lower than in the observations and case 1. Further, the predicted ground/skin temperature in case 3 is higher by 4.5 K than in the observations, causing Θ_v in the lowest layer to be 4 K higher.

The observed vertical distribution of water vapour mixing ratio (q) at 1300 LT and corresponding model predictions for cases 1 through 3 are shown in Figure 1d. The altitude ($\sim$1300 m AGL) at which a steep gradient in the observed q is present indicates the probable depth of the mixed layer at 1300 LT. Note that the case 2 predicted mean q in the ABL is closer to the observations than that in case 1 (control simulation), because latent heat fluxes are higher in case 2. The predicted mean q in the ABL in case 3 is lower than the observations by 4 g kg^{-1} due to the prediction of relatively low latent heat fluxes.

Figures 1a–1d show that uncertainty in the specification of soil texture can have significant effects on the simulated structures of the ABL over a vegetated region.

4.2. Initial soil moisture

Evaporation from bare soil and transpiring canopies is largely controlled by the moisture content of the soil. As discussed earlier, the Noilhan–Planton scheme includes two soil layers (top layer 0.01 m thick, bottom layer 1.0 m thick). Layer 1 directly contributes to evaporation from the land surface; layer 2 contributes to evapotranspiration from plants. Also, the moisture in layer 2 can be changed through seepage to or from layer 1 and vice versa. Thus, turbulent heat fluxes are also controlled by the amount of moisture present in the soil layers.

Mahfouf (1990) demonstrated the importance of soil moisture specification in ABL studies using data from HAPEX-MOBILHY (André et al. 1986). He found that soil moisture affects surface scalars such as relative humidity and temperature, thus influencing the latent and sensible heat fluxes. Similar results were found by Siebert et al. (1992). Jacquemin and Noilhan (1990) identified soil moisture availability as the most significant parameter in the biospheric setup for short-range predictions. Similarly, Niyogi et al. (1996) found that errors in the specification of deep soil moisture do not disappear in the ABL models, highlighting the importance of accurate specification of soil moisture. Shaw (1983) and Mascart et al. (1991) showed that soil moisture availability dictates the evapotranspirative flux for various landscapes. Over the FIFE site Pleim and Xiu (1995) found that the difference between the predicted maximum ABL depths in the simulations using wilting point and field capacity soil moisture values was about 1 km. They also found that the surface temperature difference between these two simulations was about 8.5 K. Kim and Stricker (1996) attempted to resolve heterogeneity in the soil moisture specifications for atmospheric models using stochastic models. Clearly, these modelling and observational studies highlight the importance and uncertainty associated with soil moisture in the meteorological perspective.

In case 1 (control simulation), observed values of the volumetric initial soil moisture used for layers 1 and 2 were 0.23 and 0.25 $m^3\ m^{-3}$, respectively. To study uncertainty effects, we conducted simulation cases 4 and 5; in case 4, initial soil moisture was specified as the field capacity value (0.322 $m^3\ m^{-3}$), while in case 5 the specified initial soil moisture was 0.240 $m^3\ m^{-3}$, ~10% higher than the wilting point value. This value (rather than the actual wilting point value) was chosen for case 5 because the soil moisture in the root zone for vegetated regions may not approach the actual wilting point value except during a drought. Performing this kind of analysis for simulations of a prolonged drought period would likely not be very useful, because estimates of initial soil moisture would be so close to the wilting point value that their level of uncertainty would probably be low.

Figure 2a shows the temporal variations in observed and predicted turbulent latent heat fluxes. In case 4, predicted latent heat fluxes closely follow the observed and case 1 values up to 1200 LT. After that time, predicted latent heat fluxes in case 4 exceed observations by ~10–70 W m^{-2}, because more initial soil moisture is available in case 4. During the entire simulation period, case 5 predicted latent heat fluxes are lower than the observations by ~10–120 W m^{-2} due to the limited availability of soil moisture. Figure 2b shows the temporal variation in observed and predicted sensible heat flux. Consistent with latent heat fluxes, predictions for case 4 are lower than observed values by ~0–60 W m^{-2} and predicted sensible heat fluxes in case 5 are higher than in the observations; the predicted maximum (244 W m^{-2}) is 97% higher than the observed maximum (124 W m^{-2}).

Observed Θ_v profiles and those predicted for cases 1, 4, and 5 at 1300 LT are shown in Figure 2c. In case 4, the mean ABL temperature is cooler than the observations by 1.75 K and the altitude of inversion at the top of the ABL is lower by ~300 m. It is interesting to note that the mean Θ_v of the mixed layer in case 5 is very similar to that in the observations. However, the ground and near-surface air temperatures are ~2 K higher than the respective observed values. Further, superadiabatic lapse rates in the surface layer in case 5 are too high when compared with the observations. Figure 2d shows observed and predicted vertical profiles of q at 1300 LT. Prediction of higher latent heat fluxes in case 4 led to a more humid boundary layer than in case 1 but still drier than in the observations. Errors present in the predicted mean q in the ABL are about -1.5, -1, and -3 g kg^{-1}, respectively, in cases 1, 4, and 5. Thus, uncertainty in the specification of initial soil moisture had a marginal to moderate effect on the simulated ABL.

It is interesting that a 40% increase over the observed initial soil moisture affected the simulated boundary layer less than a much smaller 4% decrease for the same parameter. This occurred because, for the area studied, evapotranspiration made up most (80%) of the total evaporation; bare ground evaporation played only a minor role. Since the observed initial soil moisture for layer 2 is above midsaturation and the observed minimum stomatal resistance is low, predicted evapotranspiration rates in case 1 are close to maximum. Thus, the 40% increase in initial soil moisture in case 4 primarily increased the bare ground evaporation,

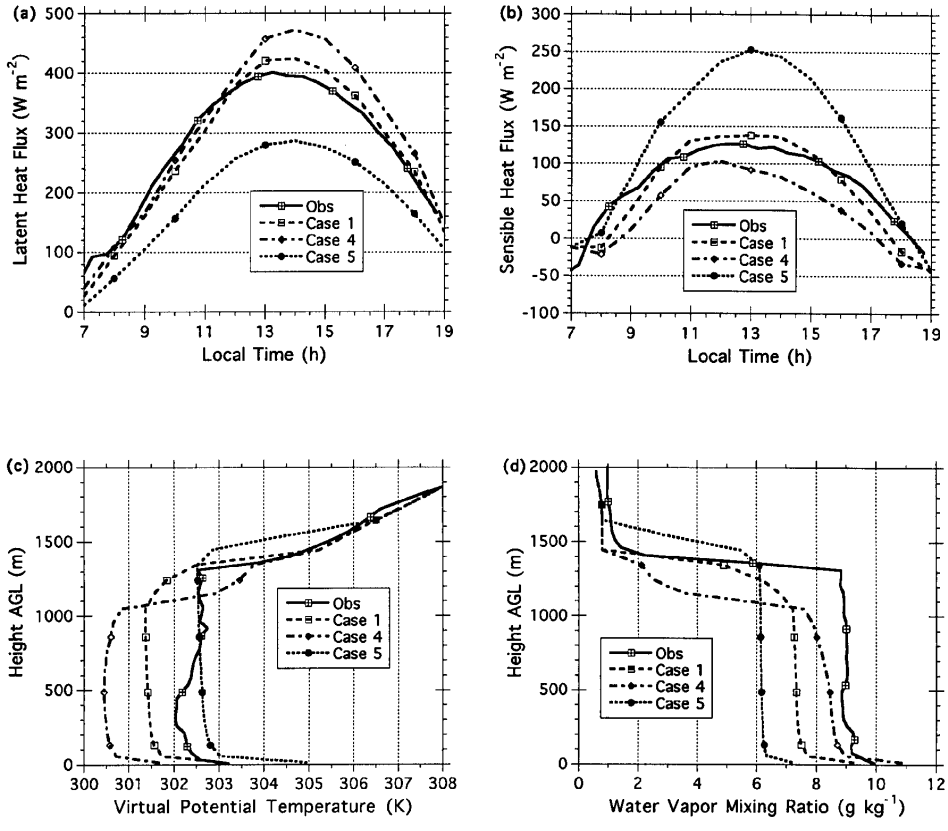

Figure 2. Observations and predictions for the initial soil moisture study: (a) temporal variation in turbulent latent heat fluxes, (b) temporal variation in turbulent sensible heat fluxes, (c) vertical variation in virtual potential temperature at 1300 LT, and (d) vertical variation in water vapour mixing ratio at 1300 LT.

resulting in only a small effect on total evaporation. On the other hand, the 4% decrease in initial soil moisture (case 5) moved it below the midsaturation value and closer to the wilting point, causing a moderate decrease in evapotranspiration and thus in total evaporation.

4.3. MINIMUM STOMATAL RESISTANCE

Minimum stomatal resistance is another parameter used in the Noilhan-Planton scheme. Evapotranspiration is controlled by valve-like structures on the leaves called stomata. An increase in stomatal resistance (decrease in conductance) in a leaf results in decreased transpiration. In the Noilhan-Planton scheme, stomatal resistance is a function of $R_{s\,\min}$, the value of minimum stomatal resistance at high solar flux over well-irrigated lands. This value varies considerably depending upon the type of vegetation; for example, the observed $R_{s\,\min}$ for maize is 40 s m^{-1} while

for oats it is 450 s m^{-1} (Jacquemin and Noilhan, 1990). Since stomatal resistance is a function of the local environment and plant-specific physiology (Farquhar and Sharkey, 1982), specification of an effective value for each gridded landscape could have errors of varying magnitude (Noilhan and Lacarrere, 1995). Even under homogeneous micrometeorological field conditions, stomatal resistance can vary widely and can be sensitive to various ambient forcings (Avissar, 1993).

Siebert et al. (1992) found that stomatal resistance largely controls the surface fluxes. Similarly, Mascart et al. (1991) (the HAPEX-MOBILHY study) found that the large stomatal resistance of the Landes forest canopy resulted in a significantly stronger sensible heat flux in both the simulations and the observations. They also found a substantial modification of the depth and structure of the ABL. Thus, uncertainty present in the stomatal resistance can influence the estimation of evapotranspiration. In simulation cases 6 and 7, minimum stomatal resistance was specified as 45 and 450 s m^{-1} respectively.

The temporal variations in observed and predicted latent heat fluxes are shown in Figure 3a. The observed $R_{s\,\min}$ used in the case 1 control simulation (60 s m^{-1}) is close to the $R_{s\,\min}$ used in case 6 (45 s m^{-1}). Thus, as expected, the decrease in the minimum stomatal resistance caused the latent heat fluxes in case 6 to be marginally higher than those in case 1. In case 7, $R_{s\,\min}$ is about ten times higher than in case 6, resulting in predicted latent heat fluxes that are about four times lower. We also noticed that bare soil evaporation is the same in all three cases but evapotranspiration varied widely, particularly in case 7. As expected from the results of earlier mesoscale studies of Mascart et al. (1991) and André et al. (1989), Figure 3b shows opposite trends in predicted sensible heat fluxes; the maximum sensible heat flux in case 7 is $\sim$2.5 times higher than in the other two cases and the observations. These features are consistent with the earlier results of Jacquemin and Noilhan (1990) for a much smaller scale as compared to Mascart et al. (1991) and André et al. (1989).

Figure 3c shows the vertical variations in observed and predicted Θ_v at 1300 LT. Consistent with the predicted heat fluxes, the mean mixed-layer virtual potential temperature is cooler by 1.75 K in case 6, and warmer by 1 K in case 7. Note that despite the large difference between the predicted turbulent heat fluxes for cases 6 and 7, the difference between their mean mixed-layer temperatures is only 2.75 K. This is because the large predicted sensible heat fluxes in case 7 are used up in mixing the air through a larger depth than in case 6, which is clearly reflected in the locations (altitudes) of the inversions in cases 6 and 7. Consistent with the predicted latent heat fluxes, the mean water vapour mixing ratio of the ABL (Figure 3d) is lower in case 7 and higher in case 6 as compared to case 1. Clearly, uncertainty in the specification of $R_{s\,\min}$ can significantly affect the simulated ABL.

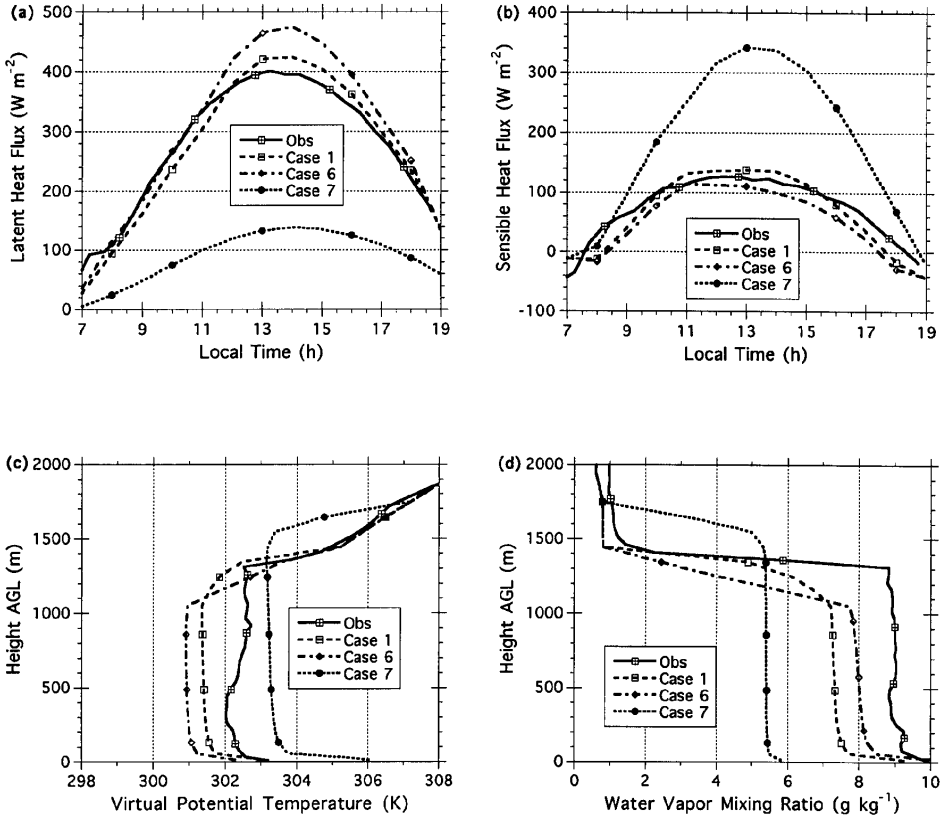

Figure 3. Observations and predictions for the minimum stomatal resistance study: (a) temporal variation in turbulent latent heat fluxes, (b) temporal variation in turbulent sensible heat fluxes, (c) vertical variation in virtual potential temperature at 1300 LT, and (d) vertical variation in water vapour mixing ratio at 1300 LT.

4.4. LEAF AREA INDEX

Leaf area index (LAI) essentially represents the normalized aerial availability of transpiring leaves. In terms of modelling surface processes, LAI can affect radiation, foliage temperature, and the maximum rainfall interception due to vegetation. In a heterogeneous landscape, the vegetation types may be similar and represented with a "constant" minimum stomatal resistance. However, LAI can vary significantly from plant to plant. Even though empirical functions can be used to estimate LAI (e.g., Dickinson et al., 1993), the accuracy of the estimates needs to be verified before they can be used in mesoscale models. Niyogi et al. (1996) showed that the Bowen ratio is influenced by changes in the LAI for a landscape. This parameter is considered important for biospheric simulations at all temporal and spatial scales (Pitman, 1994; da Rocha et al., 1996; Jacquemin and Noilhan, 1990; Acs et al. 1991; Jacobs and DeBruin, 1992). Siebert et al. (1992) found that, compared with

the influences of other surface parameters, variations in the LAI had a weak effect on the model simulations. To study the effects of uncertainty in the specification of LAI, we performed two simulations . Case 1 (control simulation) used an observed LAI of 1.9; cases 8 and 9 used LAIs of 1.0 (typical for meadows) and 3.0 (typical for farmlands), respectively.

Figure 4a gives the temporal variation in the observed and predicted turbulent latent heat fluxes. In general, predicted latent heat fluxes in all simulations follow the observations closely. The difference between the maximum latent heat flux predicted in cases 8 and 9 is only 70 W m^{-2}. Again, opposite trends in the predicted sensible heat fluxes are seen (Figure 4b). Note that the predicted sensible heat fluxes in case 9 closely match the observations, but latent heat flux predictions do not. This is similar to cases 4 and 5 (Figure 2), where predicted fluxes differed from observations but Θ_v in case 5 and q in case 6 were close to the observations. The presence of this kind of feature – one or more of the predicted variables closely resemble the observations while the rest do not – is clearly due to uncertainty in the specification of surface parameters. This suggests that some or all of the surface parameter values used in case 1 (control simulation) need to be changed to achieve better predictions, which again points to the presence of uncertainty in the case 1 surface parameters.

Observed and predicted vertical variations in Θ_v at 1300 LT are shown in Figure 4c. Differences among the predicted Θ_v in the three cases are less than $\sim$0.5 K. Similar results are seen in the predicted water vapour mixing ratio (Figure 4d). Overall, comparison of cases 8 and 9 shows that, even with a 200% increase (tripling) in LAI from case 8 to case 9, uncertainty in the LAI has only a marginal effect on the model simulations.

4.5. VEGETATION COVER

Vegetation cover acts as a shield, intercepting solar radiation before it reaches the ground, and it influences evapotranspiration. In addition, vegetation cover intercepts rainfall reaching the surface, leading to additional evaporation from the wet parts of the canopy; however, since cloud formation and associated rainfall processes are not modelled in the simulations, the effects of the additional evaporation are absent. Siebert et al. (1992) found that increased vegetation cover resulted in damping the diurnal temperature wave, affecting the structure of the ABL. Jacquemin and Noilhan (1990) also found that in their model simulations vegetation cover was the most sensitive parameter among the surface parameters. To quantify the effects of uncertainty in the specification of vegetation cover, we performed two more simulations.

Case 1 used an observed vegetation cover value of 99%, while cases 10 and 11 used 66% and 33%, respectively. Figure 5a shows the temporal variation in the observed and predicted latent heat fluxes. A decrease in vegetation cover from 99% to 66% results in decreased latent heat fluxes by $\sim$10–40 W m^{-2} compared

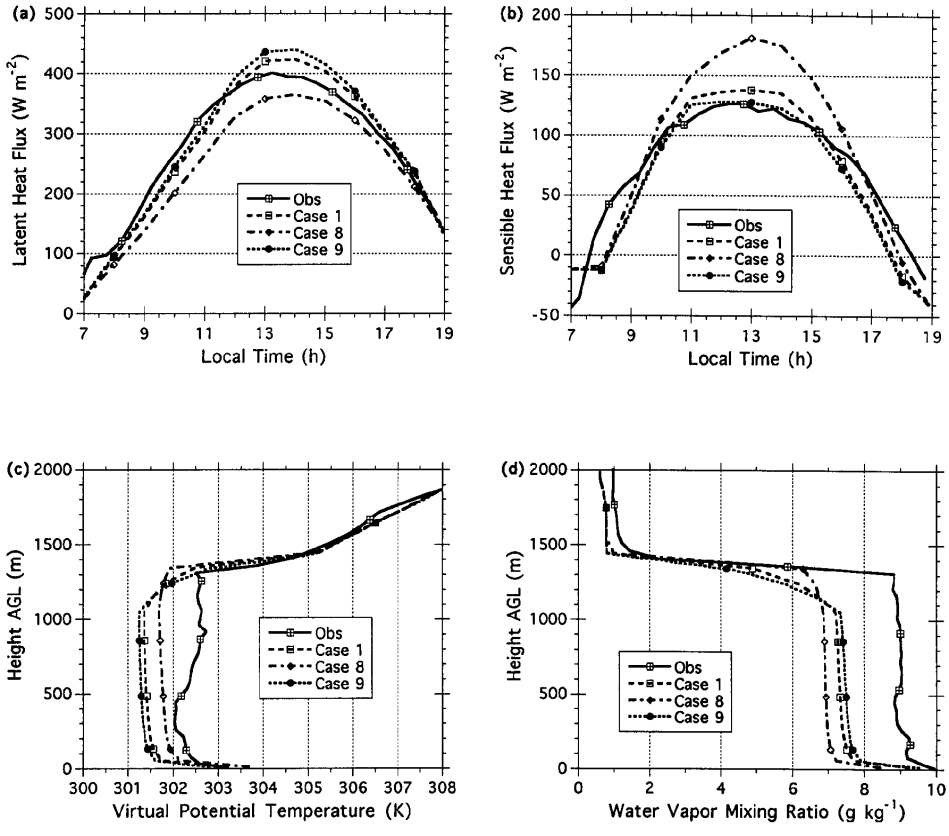

Figure 4. Observations and predictions for the leaf area index study: (a) temporal variation in turbulent latent heat fluxes, (b) temporal variation in turbulent sensible heat fluxes, (c) vertical variation in virtual potential temperature at 1300 LT, and (d) vertical variation in water vapour mixing ratio at 1300 LT.

to the observations. A further decrease to 33% results in a continued decrease in latent heat fluxes, with the maximum reaching only 260 W m^{-2}. Opposite trends occur in the predicted sensible heat fluxes (Figure 5b). In case 11, the predicted maximum sensible heat flux (244 W m^{-2}) is 97% higher than in the observations (124 W m^{-2}). A similar feature is explained in greater detail by Anthes (1984) and Mahfouf et al. (1987) for alterations in heat flux and humidity transport. The observed and predicted Θ_v profiles at 1300 LT (Figure 5c) show that, even though errors in the predicted mean Θ_v of the mixed layer were smaller in cases 10 and 11 than in case 1 (compared with observations), the superadiabatic lapse rates in the surface layer are abnormally high in cases 10 and 11. The simulated profiles of water vapour mixing ratio in cases 10 and 11 (Figure 5d) indicate increased prediction errors as the vegetation cover percentage decreases from the observed value of 99%.

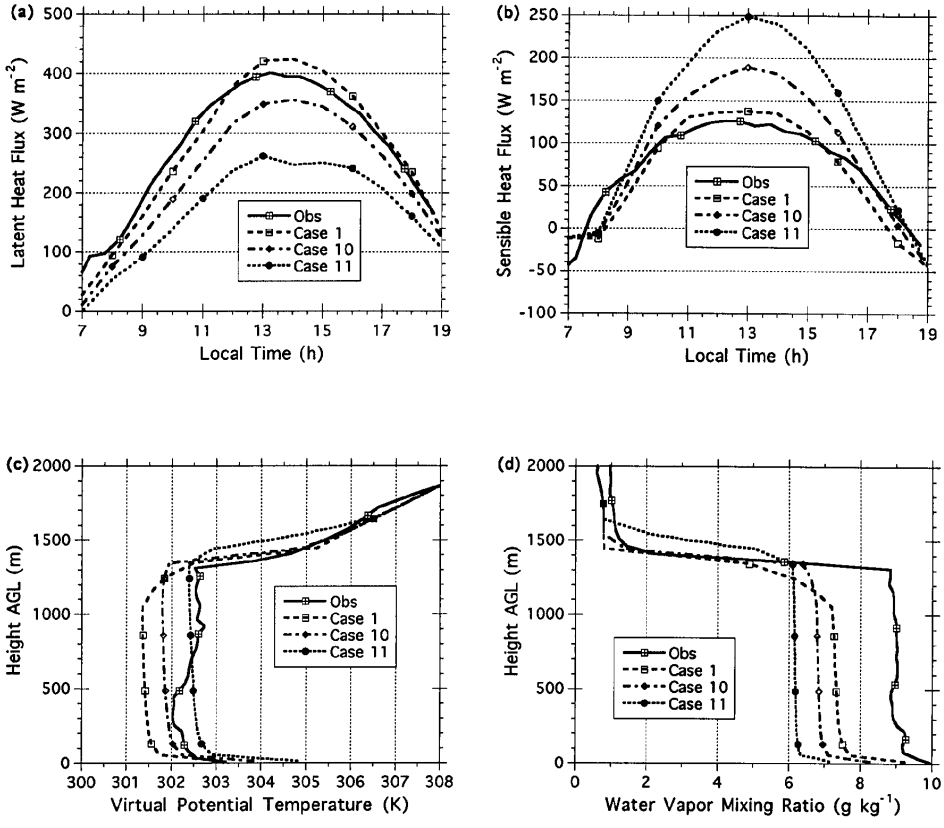

Figure 5. Observations and predictions for the vegetation cover study: (a) temporal variation in turbulent latent heat fluxes, (b) temporal variation in turbulent sensible heat fluxes, (c) vertical variation in virtual potential temperature at 1300 LT, and (d) vertical variation in water vapour mixing ratio at 1300 LT.

Overall, a 66% reduction in the observed vegetation cover (to 33%) has a moderate effect on the simulated boundary layer, consistent with the findings of Pitman (1994). The effect could be more dramatic if, for example, a 100% error existed in the specification of vegetation cover (e.g., specification of desert conditions for a dense forest region), since simulated evapotranspiration could be at one of the extremes. These uncertainties related to vegetation cover could also be significant under low soil moisture availability conditions typical of arid or semi-arid regions (Niyogi et al., 1996).

4.6. VERTICAL DISTRIBUTION OF HORIZONTAL WINDS

We also analyzed the effects of uncertainty in the specification of surface parameters on the predicted profiles of horizontal winds. Figures 6a and 6b show the vertical profiles of observed u-wind (eastward wind) and v-wind (northward wind) at 1300

LT and the corresponding predicted winds from cases 1 through 11. Observed u-winds show the presence of vertical shear, indicating the absence of well-mixed layers, while observed v-winds show negligible vertical wind shear except near the surface (0 to 100 m). In general, differences among the predicted winds for all cases are negligible below 1000 m altitude. Some minor differences among the predicted winds exist above this altitude; this occurs because the simulated depths of the boundary layer differ among the simulations, affecting the predicted wind profiles through vertical mixing. It is interesting to note that, unlike the thermodynamic parameters, the predicted wind profiles do not show dramatic variations among the cases. This result is very similar to the findings of Mascart et al. (1991) , who also found that sensitivity simulation results indicated no clear modification of the wind fields. In the absence of advective transport processes , this result can be attributed to the following: (1) turbulent momentum fluxes in the lowest layer are always negative, since momentum is continuously lost to the ground; and (2) turbulent momentum fluxes are small, unlike turbulent heat fluxes near the surface. Thus, in the 1-D simulations, uncertainty in the specification of surface parameters has an insignificant effect on the simulated horizontal wind fields.

4.7. VERTICAL DISTRIBUTION OF TURBULENT HEAT FLUXES

Many large-eddy simulation results (e.g., Wyngaard and Brost, 1984) have indicated that under quasi-steady state conditions, a scalar flux (such as turbulent sensible heat flux) has a linear vertical profile within the mixed layer. Also under these conditions, the mean vertical gradient of that scalar is steady over time. Any curvature (or deviation from linear variation) in the scalar flux profile is a direct result of temporal changes in the mean vertical gradient of the scalar. It is interesting to study the effects of uncertainty in surface parameters on the vertical distributions of predicted turbulent fluxes. Figure 7a gives the vertical variations in turbulent sensible heat flux obtained using Equation (15) for cases 1 through 11 at 1300 LT (since observational data are not available, only model predictions are shown). In all of the cases, the estimated turbulent sensible heat flux profiles above the surface layer (above $\sim$100 m) indicate a linear variation within the mixed layer. The prediction of temporally varying sensible heat fluxes near the surface and the presence of a weak vertical mixing cause gradients in the surface layer, resulting in deviations from the linear profiles seen in the mixed layer. Also, the negative sensible heat fluxes in each case's interfacial layer (the layer between the two altitudes where sensible heat flux crosses zero) are caused by the entrainment of "potentially" warmer air from the free atmosphere into the mixed layer.

The altitude of the maximum negative sensible heat flux is different for each case, reflecting the various depths of the simulated boundary layers. For case 3, predicted near-surface sensible heat flux and its maximum negative value in the interfacial layer are both larger than the respective values for the rest of the cases. However, this kind of correlation between the sensible heat fluxes near the surface

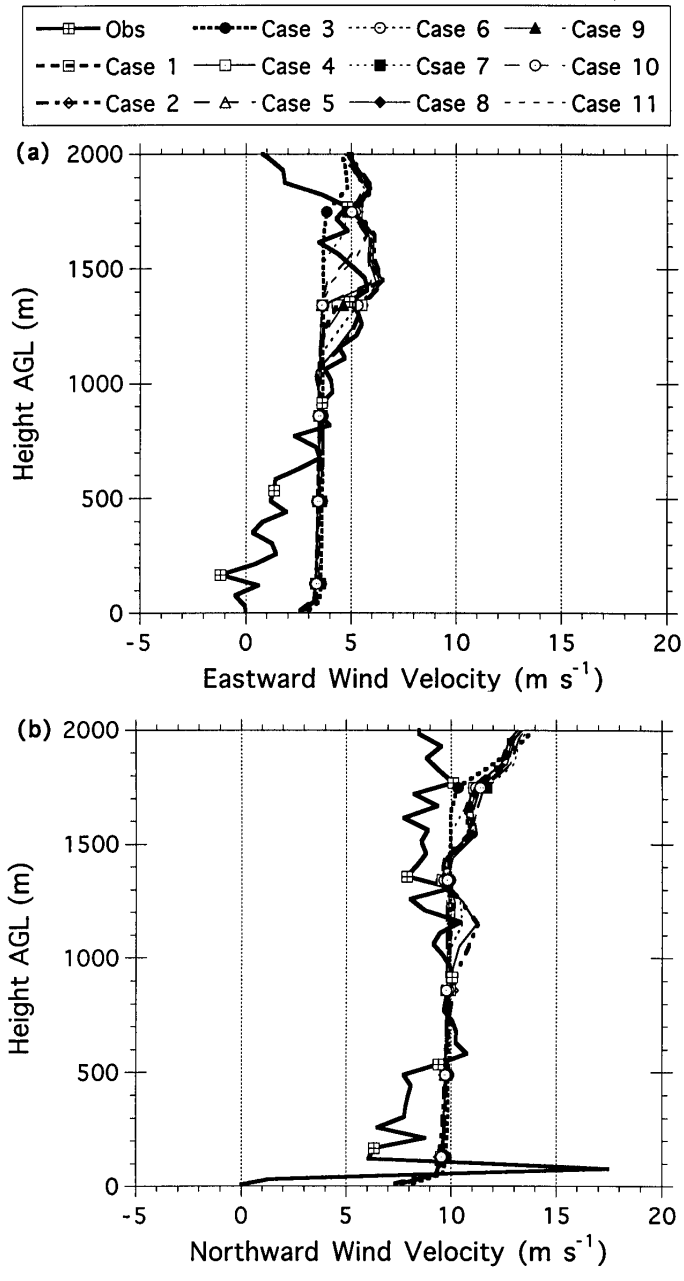

Figure 6. Vertical variation in observed and predicted (cases 1 through 11) wind velocity: (a) eastward (u-wind) and (b) northward (v-wind).

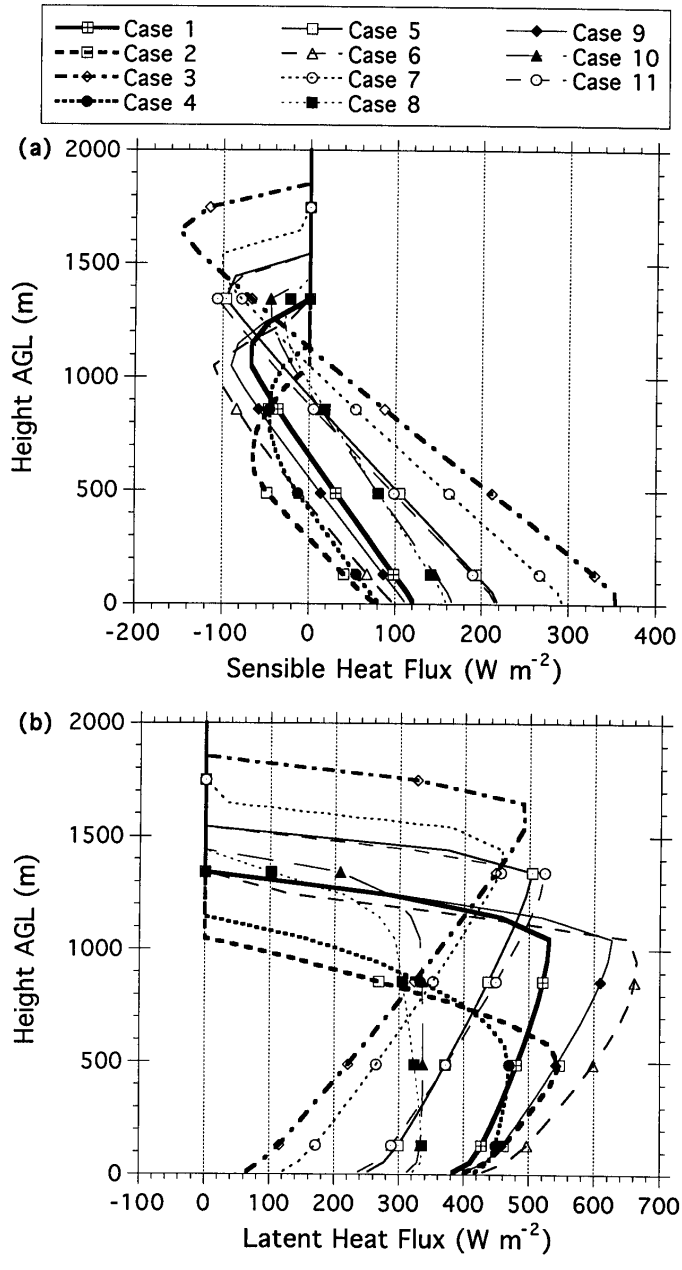

Figure 7. Vertical variation in (a) turbulent sensible heat fluxes and (b) turbulent latent heat fluxes predicted in cases 1 through 11.

and in the interfacial layer does not always occur. For example, the near-surface sensible heat fluxes in cases 6 and 11 are quite different ($\sim$100 W m^{-2} versus $\sim$300 W m^{-2}), but the maximum negative sensible heat flux in the interfacial layer for these two cases is almost the same (about -100 W m^{-2}). Overall, it can be seen that vertical gradients in the estimated sensible heat flux profiles in the boundary layer are strongly influenced by variations in the surface characteristics.

Figure 7b, analogous to Figure 7a, shows the vertical variations in turbulent latent heat fluxes. As with the sensible heat fluxes, the latent heat fluxes in the surface layer differ from those in the mixed layer. Notice that the maximum latent heat fluxes in all cases are located in the respective interfacial layers, even though evaporation exists only near the surface. As the ABL grows to higher altitudes, drier air is entrained from the free atmosphere into the mixed layer. Therefore, to maintain well-mixed layers in the ABL, large amounts of moisture must be pumped up into the upper layers within the ABL. Consequently, large latent heat fluxes are predicted in the interfacial layer (close to the top of the ABL).

The effects of uncertainty in the specification of surface characteristics are apparent in the vertical distributions of turbulent heat fluxes. The differences in the predicted ground temperature (not shown) caused by the surface parameter uncertainties can in turn cause variations in the predicted availability of chemical fluxes (e.g., biogenic emission fluxes) of reactive species. In air quality modelling studies, this could strongly influence chemical transformations and the resulting concentrations of chemical species. Thus, uncertainty in the representation of surface characteristics may also affect the results of air quality modelling studies.

4.8. Evolution of the depth of the boundary layer

Finally, we study the effects of uncertainty in the specification of the five surface parameters on the simulated ABL depth. In meteorological modelling, ABL depth is one of the important parameters that determines the vertical mixing of meteorological parameters within the ABL, and the altitude of the base of the clouds. In air quality modelling studies, proper specification of ABL depth is crucial because it determines the depth of the dilution of pollutants. Thus, the accuracy of model predictions in these two applications largely depends on the accuracy of the predicted depth of the ABL. For observations, we used altitudes of the top of the inversion that were obtained from ground-based SODAR measurements. Figure 8 shows the observed depth of the ABL and the depth predicted for cases 1 through 11. The maximum predicted ABL depth occurs in case 3, indicating the dominance of soil texture in controlling the evolution of the ABL. The effects of uncertainty in the specification of minimum stomatal resistance (case 7) are at a similar level. The effects of low initial soil moisture (case 5) and low vegetation cover (case 11) are very similar to each other, while less than the effects shown in cases 3 and 7. Low leaf area index (case 8) and moderate vegetation cover (case 10) have effects on the predicted ABL that are similar to each other but lower than the effects in cases

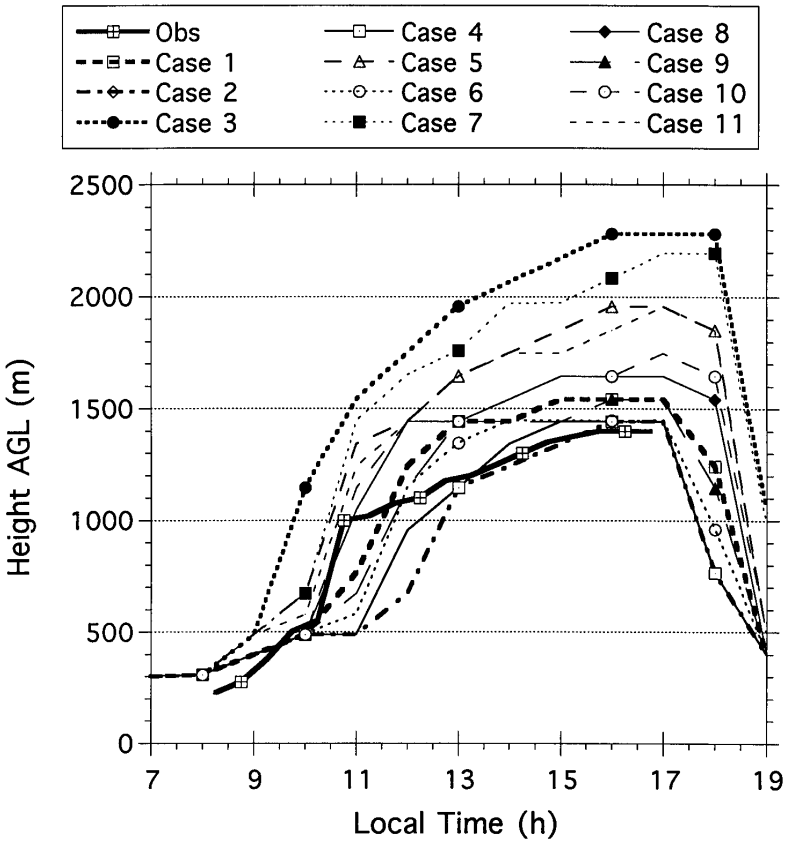

Figure 8. Temporal evolution of the estimated and predicted (cases 1 through 11) depth of the boundary layer.

5 and 11. In the rest of the cases (2, 4, 6, and 9), the effects are evident primarily during the growth phase of the ABL. After 1400 LT, when the ABL has reached its maximum depth, differences among the predicted depths of the ABL in these four cases are not significant.

5. Summary and Conclusions

We used a 1-D soil-vegetation-boundary-layer model to study how uncertainty in the specification of surface characteristics affects the processes and structure of a simulated ABL. Full interaction between the land surface and the atmosphere was allowed using a soil-vegetation scheme and a nonlocal-closure boundary-layer scheme. FIFE observed surface characteristics and atmospheric data were used to simulate the observed boundary-layer processes in the control simulation. In the other simulations, we specified different values of five surface parameters: soil

texture, initial soil moisture, minimum stomatal resistance, leaf area index, and vegetation cover.

The results obtained in this study are qualitatively consistent with other studies at various scales. Though our study is based on a specific FIFE case, we have established a simple quantification of the magnitude of prediction errors. This can have direct implications in interpreting boundary-layer outcomes from air quality and meteorological models. Since the study utilized a coupled atmosphere-land surface scheme, the results can be extended, at least qualitatively, to different scales, as outlined by Pitman (1994) and da Rocha et al. (1996). The outcomes can also be paired with those from other studies representing different landscapes to assess the effort required to generate accurate inventories for various parameters. For parameters that can result in large prediction errors, such as stomatal resistance, a detailed inventory with a high level of confidence is needed.

Table III presents a summary of the findings for the 11 cases in terms of predicted maximum value minus observed maximum value for turbulent heat fluxes, and predicted mean mixed-layer value minus observed mean mixed-layer value for virtual potential temperature and water vapour mixing ratio. The Table also presents a qualitative judgment about the overall level of the effect of parameter specification uncertainty on the predicted ABL. Our results show that uncertainty in the specification of some of these surface processes can significantly affect the simulated ABL processes and structure, which has implications for both meteorological and air quality simulation modelling.

Table III shows that under certain conditions uncertainties in the specification of soil texture and of minimum stomatal resistance (hence stomatal resistance; both are determined by the land use specified) can significantly affect the simulated ABL. Both evaporation and evapotranspiration are greatly influenced by uncertainties in the specification of these two surface characteristics, because water retention capacity varies widely with soil texture, and transpiration is controlled by stomatal conductance/resistance.

Uncertainty in the soil moisture affected the simulated ABL less, but still produced a moderate effect. For reasons noted earlier, increasing the soil moisture 40% (to field capacity) produced only a marginal effect, but decreasing it by only 4% (to 10% above the wilting point value) had a much stronger effect. The outcome of the reduction was a prediction of superadiabatic lapse rates that were too high when compared with the observations; strong superadiabatic lapse rates can trigger the formation of shallow and/or deep clouds if the atmosphere is convectively unstable.

A large decrease in the vegetation cover (66%) resulted in the prediction of higher superadiabatic lapse rates compared with the observations. The large decrease also produced a moderate effect in the simulated boundary layer. However, as noted earlier, a 100% uncertainty in the vegetation cover (unlikely to occur, but possible) could lead to significant prediction errors. Finally, both a decrease and an increase in the leaf area index resulted in only marginal differences between the simulated and the observed structures of the ABL.

Table III
Summary of the findings for the 11 cases

Parameter specified	Case number	Parameter type/value used	Error in L^*	Error in S^*	Error in Θ_v †	Error in in $q^\dagger$	Overall level of uncertainty effect on ABL
Soil texture	Case 1	Silty clay loam (observations)	+25	+10	−1.25	−1.5	NA (control simulation)
	Case 2	Loamy sand	+40	−30	−2	−1	Marginal
	Case 3	Clay	−300	+300	+1.5	−4	Significant
Initial soil moisture ($m^3\ m^{-3}$)	Case 1	0.230 (layer 1) and 0.250 (layer 2) (observations)	+25	+10	−1.25	−1.5	NA (control simulation)
	Case 4	0.322 (field capacity)	+70	−60	−1.75	−1	Marginal
	Case 5	0.240 (∼10% higher than wilting point)	−120	+120	+0.5	−3	Moderate
Min. stom. resistance ($s\ m^{-1}$)	Case 1	60 (tall grass) (observations)	+25	+10	−1.25	−1.5	NA (control simulation)
	Case 6	40 (maize)	+80	−20	−1.75	−1	Marginal
	Case 7	450 (oats)	−260	+220	+1	−4	Significant
Leaf area index	Case 1	1.9 (observations)	+25	+10	−1.25	−1.5	NA (control simulation)
	Case 8	1.0 (meadows)	−30	+50	−0.75	−2	Marginal
	Case 9	3.0 (farmlands)	+40	+5	−1.3	−1.25	Marginal
Vegetation cover	Case 1	0.99 (observations)	+25	+10	−1.25	−1.5	NA (control simulation)
	Case 10	0.66	−40	+60	−0.5	−2	Marginal
	Case 11	0.33	−140	+120	+0.5	−3	Moderate

*Predicted maximum – observed maximum.
†Predicted mean mixed-layer value – observed mean mixed-layer value.

We also found that the uncertainties in the parameters studied here significantly affected the vertical distribution of turbulent heat fluxes. Resulting differences in the predicted ground temperatures could lead to different estimates of reactive chemical fluxes, affecting simulated chemical concentrations. Unlike turbulent heat fluxes, predicted turbulent momentum fluxes in all simulations were very similar and led to negligible effects on the simulated horizontal wind fields. The predicted maximum boundary-layer depths of the simulated ABLs showed considerable variation among the 11 simulations, ranging from about 1400 to 2300 m.

Acknowledgments

The information in this document has been funded in part by the United States Environmental Protection Agency under cooperative agreement CR-823628 to MCNC, and it has been approved for publication by MCNC. It has also been funded in part by the Division of Atmospheric Sciences, National Science Foundation Grant ATM 9212636, and in part by the U.S. Department of Energy, Atmospheric Radiation Measurement Program under contract 09157-A-Q1 with Pacific Northwest Laboratories, to North Carolina State University. The authors thank Ms. Jeanne Eichinger for her editorial assistance.

References

Acs, R., Mihailocic, D. T., and Rajkovic, B.: 1991, 'A Coupled Soil Moisture and Surface Temperature Prediction Model', *J. Appl. Meteorol.* **30**, 812–822.

Alapaty, K., Pleim, J. E., Raman, S., Niyogi, D. S., and Byun, D. W.: 1997, 'Simulation of Atmospheric Boundary-layer Processes Using Local- and Nonlocal-closure Schemes', *J. Appl. Meteorol.* **36**, 214–233.

Andre, J.-C., Bougeault, Ph., Mahfouf, J.-F., Mascart, P., Noilhan, J., and Pinty, J.-P.: 1989, 'Impact of Forest on Mesoscale Meteorology', *Philos. Trans. R. Soc. London Ser. B.* **324**, 408–422.

Andre, J. C., Goutorbe, J. P., and Perrier, A.:1986, 'HAPEX-MOBILHY: A Hydrologic Atmospheric Experiment for the Study of Water Budget and Evaporation Flux at the Climate Scale', *Bull. Amer. Meteorol. Soc.* **67**, 138–144.

Anthes, R. A., Hsie, E.-Y., and Kuo, Y.-H.: 1987, 'Description of the Penn State/NCAR Mesoscale Model Version 4 (MM4)', NCAR Tech. Note, NCAR/TN-282+STR, 66 pp.

Anthes, R. A.: 1984, 'Enhancement of Precipitation by Mesoscale Variations in Vegetative Covering and Semiarid Regions', *J. Climate Appl. Meteorol.* **23**, 541–553.

Avissar, R.: 1993, 'Observations of Leaf Stomatal Conductance at the Canopy Scale: An Atmospheric Modeling Perspective', *Boundary-Layer Meteorol.* **64**, 127–148.

Businger, J. A., Wyngaard, J. C., Izumi, Y., and Bradley, E. F.: 1971, 'Flux-profile Relationship in the Atmospheric Surface Layer', *J. Atmos. Sci.* **28**, 181–189.

Clapp, R. B. and Hornberger, G. M.: 1978, 'Empirical Equations for Some Hydraulic Properties', *Water Resour. Res.* **14**, 601–604.

da Rocha, H., Nobre, C. A., Bonatti, J. P., Wright, I. R., and Sellers, P. J.: 1996, 'A Vegetation-atmosphere Interaction Study for Amazonia Deforestation Using Field Data and a Single Column Model', *Quart. J. Roy. Meteorol. Soc.* **122**, 567–594.

Deardorff, J.: 1978, 'Efficient Prediction of Ground Surface Temperature and Moisture, with Inclusion of a Layer of Vegetation', *J. Geophys. Res.* **83**, 1889–1903.

Dickinson, R. E., Henderson-Sellers, A., and Kennedy, P. J.: 1993, 'Biosphere-Atmosphere Transfer Scheme (BATS) Version 1e as Coupled to the NCAR Community Climate Model', NCAR Tech. Note, NCAR/TN-387+STR, 72 pp.

Ek, M. and Cuenca, R. H.: 1994, 'Variation in Soil Parameters: Implications for Modeling Surface Fluxes and Atmospheric Boundary-Layer Development', *Boundary-Layer. Meteorol.* **70**, 369–383.

Farquhar, G. D. and Sharkey, T. D.: 1982, 'Stomatal Conductance and Photosynthesis', *Ann. Rev. Plant Physiol.* **33**, 317–345.

Henderson-Sellers, A.: 1993, 'A Factorial Assessment of the Sensitivity of the BATS Land-surface Parameterization Scheme', *J. Climate* **6**, 227–247.

Jacobs, C. M. J. and de Bruin, H. A. R.: 1992, 'The Sensitivity of Regional Transpiration to Land Surface Characteristics: Significance of Feedback', *J. Climate* **5**, 683–698.

Jacquemin, B. and Noilhan, J.: 1990, 'Sensitivity Study and Validation of Land Surface Parameterization Using the HAPEX-MOBILHY Data Set', *Boundary-Layer Meteorol.* **52**, 93–134.

Kim, C. P. and Stricker, J. N.: 1996, 'Consistency of Modeling the Water Budget Over Long Time Series: Comparison of Simple Parameterizations and a Physically Based Model', *J. Appl. Meteorol.* **35**, 749–760.

Mahfouf, J.-F., Richard, E., and Mascart, P.: 1987, 'The Influence of Soil and Vegetation on the Development of Mesoscale Circualtions', *J. Climate and Appl. Meteorol.* **26**, 1483–1495.

Mahfouf, J.-F.: 1990, 'A Numerical Simulation of the Surface Moisture Budget During HAPEX-MOBILHY', *Boundary-Layer Meteorol.* **53**, 201–222.

Mascart, P., Taconet, O., Pinty, J-P., Ben, M., and Mehrez, M. B.: 1991, 'Canopy Resistance Formulation and Its Effect in Mesoscale Models: A HAPEX Perspective', *Agric. For. Meteorol.* **54**, 319–351.

McCumber, M. C. and Pielke, R. A.: 1981, 'Simulation of the Effects of Surface Fluxes of Heat and Moisture in Mesoscale Numerical Model. Part I: Soil Layer', *J. Geophys. Res.* **86**, 9929–9938.

Mihailvic, D., de Bruin, H. A. R., Jeftic, M., and van Dijken, A.: 1992: 'A Study of the Sensitivity of Land Surface Parameterizations to the Inclusion of Different Fractional Covers and Soil Textures', *J. Appl. Meteorol.* **31**, 1477–1487.

Monin, A. S. and Yaglom, A. M.: 1971, 'Statistical Fluid Mechanics', Vol. I, MIT Press, pp. 468–504.

Niyogi, D. S., Raman, S., Alapaty, K., and Han, J.: 1996, 'A Dynamic Statistical Experiment for Atmospheric Interactions', *Environ. Mod. Assess.(A)*. Submitted.

Noilhan, J. and Lacarrere, P.: 1995, 'GCM Gridscale Evaporation from Mesoscale Modeling', *J. Climate* **8**, 206–217.

Noilhan, J. and Planton, S.: 1989: 'A Simple Parameterization of Land Surface Processes for Meteorological Models', *Mon. Wea. Rev.* **117**, 536–549.

Pitman, A. J., Henderson-Sellers, A., and Yang, Z.-L.:1990, 'Sensitivity of Regional Climates to Localized Precipitation in Global Models', *Nature* **346**, 734–737.

Pitman, A. J.: 1994, 'Assessing the Sensitivity of a Land-surface Scheme to the Parameter Values Using a Single Column Model', *J. Climate* **7**, 1856–1869.

Pleim, J. E. and Xiu, A: 1995, 'Development and Testing of a Surface Flux and Planetary Boundary-Layer Model for Applications in Mesoscale Models', *J. Appl. Meteorol.* **34**, 16–32.

Sellers P. J., Hall, F. G. , Asrar, G., Strebel, D. E. , and Murphy, R. E.: 1992, 'An Overview of the First International Satellite Land Surface Climatology Project (ISLSCP) Field Experiment (FIFE)', *J. Geophys. Res.* **97**, 18,345–18,371.

Sellers, P. J., Mintz, Y., Sud, Y., and Dalcher, A.:1986, 'The Design of a Simple Biosphere Model (SiB) for Use Within General Circulation Models', *J. Atmos. Sci.* **43**, 505–531.

Shaw, R. H.:1983, 'Soil Moisture and Moisture Stress Prediction for Corn in a Western Corn Belt State', *Korean J. Crop Sci.* **28**, 1–10.

Siebert, J., Sievers, U., and Zdunkowski, W.:1992, 'A One-dimensional Simulation of the Interaction Between Land Surface Processes and the Atmosphere', *Boundary-Layer Meteorol.* **59**, 1–34.

Stull, R. B. and Driedonks, A. G. M.: 1987, 'Applications of the Transilient Turbulence Parameterization to Atmospheric Boundary-Layer Simulations', *Boundary-Layer Meteorol.* **40**, 209–239.

Sud, Y. C., and Smith, W. E.:1985, 'The Influence of Surface Roughness of Deserts on the July Circulation – A Numerical Study', *Boundary-Layer Meteorol.* **33**, 15–49.

Wetzel, P. and Chang, J. T.:1987, 'Concerning the Relationship Between Evapotranspiration and Soil Moisture', *J. Climate Appl. Meteorol.* **26**, 18–27.

Wetzel, P. and Chang, J. T.:1988, 'Evapotranspiration from Nonuniform Surface: A First Apporach for Short term Numerical Weather Prediction', *Mon. Wea. Rev.* **116**, 600–621.

Wyngaard, J. and Brost, R. A.: 1984, 'Top-down and Bottom-up Diffusion of a Scalar in the Convective Boundary Layer', *J. Atmos. Sci.* **41**, 102–112.